

# A 3D LIDAR RECONSTRUCTION APPROACH FOR VEGETATION DETECTION IN POWER TRANSMISSION NETWORKS

Yi Ma<sup>a</sup>, Fangrong Zhou<sup>a</sup>, Gang Wen<sup>a</sup>, Hao Gen<sup>a</sup>, Ran Huang<sup>a</sup>, Qi Wu<sup>b,\*</sup>, Ling Pei<sup>b</sup>

<sup>a</sup>Electric Power Research Institute, Yunnan Power Grid Company Ltd., Kunming, China -  
42971995@qq.com, 42783590@qq.com, 1192381484@qq.com, whugenghao@163.com, 50276157@qq.com

<sup>b</sup>School of Electronic Information and Electrical Engineering, Shanghai Jiao Tong University, Shanghai, China -  
(robotics.qi, ling.pei)@sjtu.edu.cn

Commission III, WG III/1

**KEY WORDS:** Vegetation Management, Tree detection, Deep Learning, Ground Plane, Localization, 3D Reconstruction.

## ABSTRACT:

Vegetation management is important to the power transmission and distribution networks. The encompassed towering tree is always the key factor of the high impedance faults(HIFs).LiDAR is an efficient way to detect trees with 3D point cloud. The classical tree detection algorithm can handle the tree with high and distinct trunk, but limited to the tree with messy trunks. While the deep-learning based detection algorithms are also suffered from the terrain noise points. In this paper, we propose an efficient LiDAR reconstruction system which can efficiently reconstruct the point cloud of surrounding vegetation without the ground plane noise. We also use different weight strategies to improve the localization accuracy. We have conducted our system on the real power network environment and the height detection result shows that our algorithm has a better accuracy and robustness compared with the classical methods.

## 1. INTRODUCTION

The surrounded vegetation is the implicit insecurity factor of the power transmission and distribution network. As the Figure 1 shows, the high impedance faults(HIFs) caused by the unlimited growing tree disables the power transmission line, which leads a huge cost to the society. To detect the height of surrounded vegetation has become an interesting topic to many researchers.

As Figure.1, the classical tree detection algorithms can only adapt to the tree which has a tall and thin trunk. It can't identify either the clustering vegetation or the bushed-like trees. There are also many researchers try to use the deep-learning methods(Ali et al., 2018, Qi et al., 2017, Milioto et al., 2019) to solve this problem. However, the training data collected from the current reconstruction system always influenced by the terrain. The shape of the ground plane under the tree always drive the detection system into failure.

In this paper, we use a typical deep learning algorithm(Qi et al., 2017) to figure out the object trees in power transmission sites. In addition, we propose a LiDAR reconstruction system, which can effectively reconstruct the power transmission site environment. The main contributions of this paper are as follows:

- Apply the concentric-zone model to extract the ground plane which can alleviate the sparse problem of point cloud especially in far areas.
- Develop a LiDAR reconstruction system with accurate localization and consistent map.

\* Corresponding author

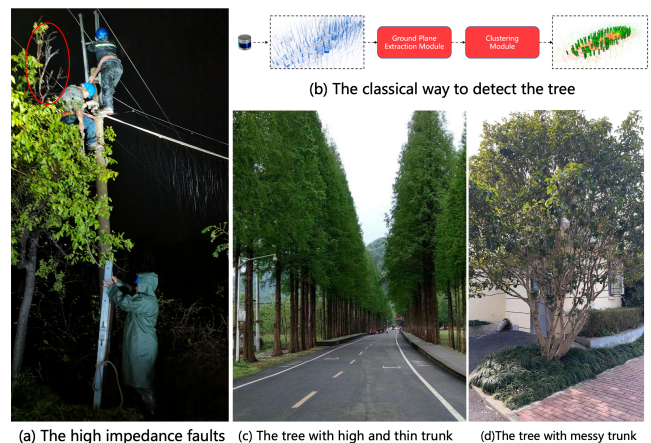


**Figure 1.** The figure(a) shows the HIF caused by the towering tree. The figure(b) shows classical pipeline of tree detection, the high and think trunk showed in figure(c) is more suitable for the clustering algorithm and the messy trunk in figure(d) always brought to the failure detection.

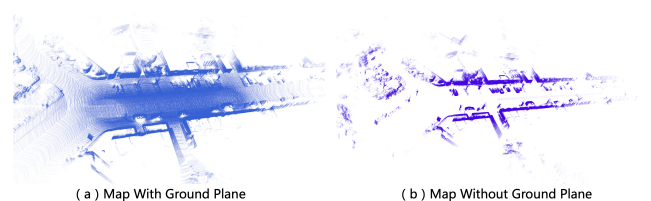


**Figure 2.** The impacts of ground plane. The left reconstruction result shows the messy ground plane points make it's hard to split out the tree information, while the right is easy to split out the tree structure without the ground plane.

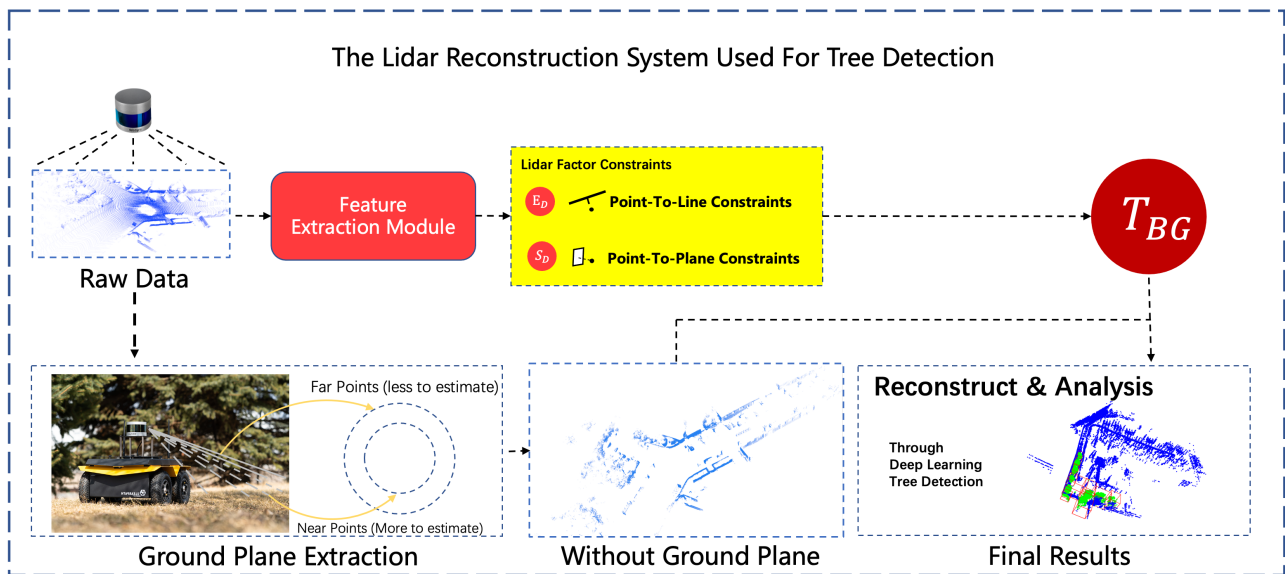


**Figure 3.** Pipeline of the reconstruction system. The whole system consist of four module: The feature extraction module, which uses the curvature to classify lidar points to point features and surf features. The ground plane extraction module which uses the concentric-zone model to filter out most messy ground plane information to build a clean reconstruction result. The lidar odometry estimation uses prior extracted features to estimate the lidar odometry. The reconstruction module uses the sensing data to build the global map. The reconstruction result is more suitable for vegetation’s height management.

- We evaluated the system in the both dataset and real power transmission environment. The results show that the system can build a clean surrounded vegetation environment and improve the height detection ability.

The rest of this paper are organized as follows. In Sect II, we discuss the related paper. In Sect.III., we show the whole pipeline of our system. The experimental results are illustrated in Sect.IV. The conclusion is presented in Sect.V.

## 2. RELATED WORK

### 2.1 Tree Detection

The vegetation’s height management is important in the electric industry. In traditional way, the workers use the GPS receiver, lidar ranger and total station to measure the tree height and location(Jelavic et al., 2021). The work is complex and has a low efficiency. For automatic detection, the researchers(Himmelsbach et al., 2010) usually remove the ground plane information and use different clusters to filter out the tree’s height. However, this method is limited to the real power site environment due to the fact that too many bushes or the clustering vegetation, more and more researcher try to use the deep-learning method to analysis the reconstruction results.

### 2.2 Ground Plane Extraction

The key process of ground plane extraction is to use the cluster patch to filter out the plane parameters. (Cheng et al., 2020, Chen et al., 2014) uses RANSAC to filter out the time-consuming plane parameters. Some researchers try to use the height of the vehicle as prior information to estimate the ground plane like(Shan and Englot, 2018, Bogoslavskyi and Stachniss, 2016). However, due to the mechanical structure of the lidar sensor, point clouds on the ground plane are not equal in the near place or the far area. In this work, following (Lim et al.,

2021)’s advice, we use the concentric model to filter out the ground plane noise, which is more suitable in the UAV platform.

### 2.3 Lidar-SLAM

With the development of the ranging sensor, the lidar slam algorithms become an widely-studied topic in the research area(Zhang and Singh, 2014, Zhang and Singh, 2017, Deschaud, 2018, Zhou et al., 2021). The most important work in the whole topic is the LOAM(Zhang and Singh, 2014, Zhang and Singh, 2017), which uses the curvature features to estimate the odometry of each scan frame. There is a series of works developed from this system(Shan and Englot, 2018, Zhou et al., 2021). The LeGo-LOAM(Shan and Englot, 2018) is one of the famous work which removes the ground plane in the feature extraction module to speed the whole process. However, the ground plane is the important factor to the z-axis constraint. In this work, we use a more efficient way to filter out the ground plane noise. The reconstruction result is more clean and valuable to the tree detection algorithm.

## 3. METHOD

The overview of the whole system is depicted in Fig.2. The whole system is splitted into four key modules: the feature extraction module, the ground plane filter module, the odometry pose-solver module and the reconstruction module. The main constraint used in this paper is the point-to-line and the point-to-plane constraints.After reconstruction, we use a deep-learning method to figure out the height of tree. The details of each module are described as follows:

### 3.1 The Feature Extraction Module

With the consideration of performance and efficiency, we adopt the feature extraction module from the LOAM algorithm(Zhang and Singh, 2014, Zhang and Singh, 2017). Using the simple but

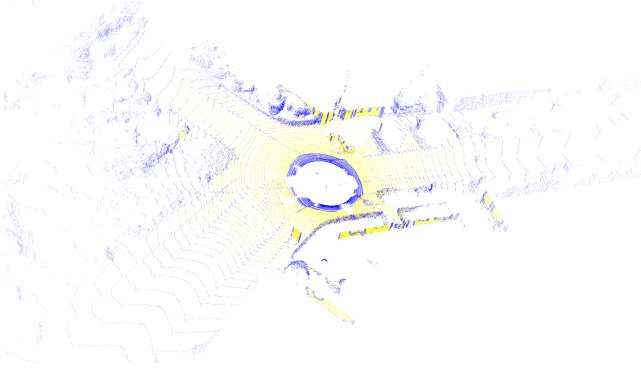


**Figure 4.** The extracted features. Point features are colored in red and surf features are colored in yellow.

effective smoothness calculation, we divide each scan into point features and surf features. The former usually represents the sharp area in the surrounding environment such as the corner of the wall, while the latter usually represents the flat area in the environment such as the flat plane. However, due to the ground plane issue, there are a lot of surf features represent the same plane, so we use the voxel filter to down sample surf features, which can speed up the whole system. The result of the extracted features is shown in Fig 4. Point features are colored in red and surf features are colored in yellow.

### 3.2 Ground Plane Extraction

The problem of ground plane extraction is depicted in Fig.5. The terrain is usually not flat, resulting the different number size in different regions. Due to the ranging pattern of the lidar sensors, there are usually less points on the far area and more points on the near place. Inspired by the work of (Lim et al., 2021), we use the concentric zone-based circle model to split the ground plane regions.

Specially, we convert the point into the polar grid representation. The polar range  $r$  is the distance of the point and the  $\phi$  is the rotation angle of the points. According to the concentric model, the point clouds are divided into multiple zones. We use  $P_m$  to represent the  $m$ -th zone of the whole points and  $N_m$  to denote the number of zones. Moreover, the  $P_m$  is divided into different bins, as follows:

$$R_{i,j,m} = \{ \mathbf{d}_k \in P_m \mid \frac{(i-1)\Delta d_m}{N_{r,m}} \leq d_k - d_{min,m} < \frac{i \cdot \Delta d_m}{N_{r,m}}, \frac{(j-1) \cdot 2\pi}{N_{\theta,m}} - \pi \leq \theta_k < \frac{j \cdot 2\pi}{N_{\theta,m}} - \pi \} \quad (1)$$

where, the  $d_k = \sqrt{x_k^2 + y_k^2}$  and the  $\theta_k = \arctan2(y_k, x_k)$ . The  $\Delta d_m$  is the boundary of each zone:

$$\Delta d_m = d_{max} - d_{min} \quad (2)$$

where the  $d_{max}$  and  $d_{min}$  represents the maximum or the minimum of each zone respectively. After splitting each region, we use the Principal Component Analysis (PCA) to figure out the ground plane parameters, which is more faster and has an acceptance accuracy.

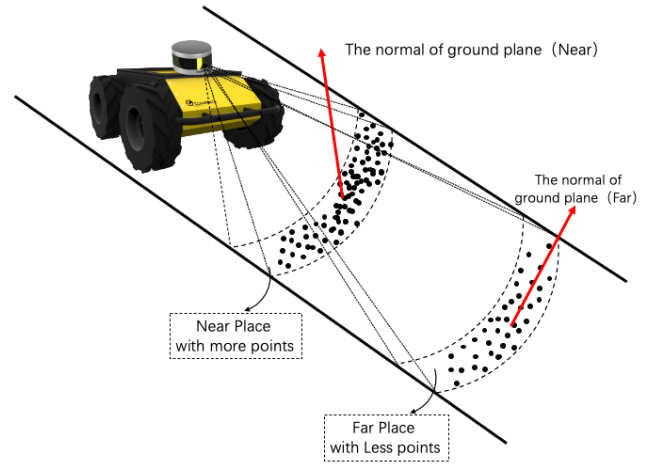


**Figure 5.** The Example of Ground Plane Estimation Proposes. The number of estimated points on different area are different.

### 3.3 Odometry Estimation

Different from the classical odometry estimation in the loam series, we use the uniform motion model to replace the scan-to-scan estimation method as the initial pose of each scan frame. Due to the low speed of UAV in power transmission networks, the uniform motion model is efficient with acceptable accuracy and we use the scan-to-map data associations as the odometry constraints to estimate the pose of each lidar scan.

The local map are stored in a KD-Tree data structure. By using the uniform motion model, the point features are projected into the map to find the nearest features in the local map. The selected features are employed as line features in the constraints. On the other hand, the corresponding surf features are usually calculated by the PCA method to get the plane parameters: the normal( $n$ ) and  $d$ . In conclusion, the whole constraint equation is:

$$J_P = p_m^T \cdot \frac{p_1^P - p_2^P}{|p_1^P - p_2^P|} \times J_p \quad (3)$$

where the

$$p_m = \frac{(\hat{p}_P - p_2^P) \times (\hat{p}_P - p_1^P)}{|(\hat{p}_P - p_2^P) \times (\hat{p}_P - p_1^P)|} \quad (4)$$

The jacobian of the surf measurement is:

$$J_S = p_n^T \cdot J_p \quad (5)$$

where the

$$p_n = \frac{(p_1^S - p_2^S) \times (p_1^S - p_3^S)^T}{|(p_1^S - p_2^S)|} \quad (6)$$

The  $J_p$  is the partion of the rotation and the translation.

$$J_p = \begin{bmatrix} \mathbf{I}_{3 \times 3} & -[\mathbf{T}_k \mathbf{p}_k] \times \\ \mathbf{0}_{1 \times 3} & \mathbf{0}_{1 \times 3} \end{bmatrix} \quad (7)$$

**Table 1.** The Ablation Study Of Lidar Features

Running Distance	Feature Type	Results
4.4km	Point Features	1.2552%
4.4km	Surf Features	1.5301%
4.4km	Point+Surf Features	1.2605%

### 3.4 Reconstruction & Point Analysis

Like the Figure 3 shows, the reconstruction map are constructed from the global coordinates parojected from the Lidar sensing points. The key of reconstruction is

$$P_{Global} = T_{GL} \cdot P_{ungroundplane} \quad (8)$$

The points without ground plane noise is cleaner to show the tree shape. The reconstruction result of a real power transmission site is like Figure 10. After we get the reconstruction result, we could use the deep learning tools to effectively split the tree and to do the height detection. Here we choose the point-net algorithm to do the following steps, the results are shown in the experiment part.

## 4. EXPERIMENTS

In this section, we will use the experimental results to prove the proposed system’s efficiency and accuracy. Our system is coded by C++ and implemented on different unix platforms. For the open dataset, the system is tested on the macbook pro with an Intel 6-core i7 processor CPU. For the latter experiments, we add the ROS interface enabling the system reconstructs the environment in real-time on our UAV platform. The time consuming of the estimation process is 50ms, which means that our algorithm has the real-time ability. To evaluate the reconstruction quality, we analyze two quality indexes. The first is the odometry drift and the second is the thickness of the reconstructed point cloud.

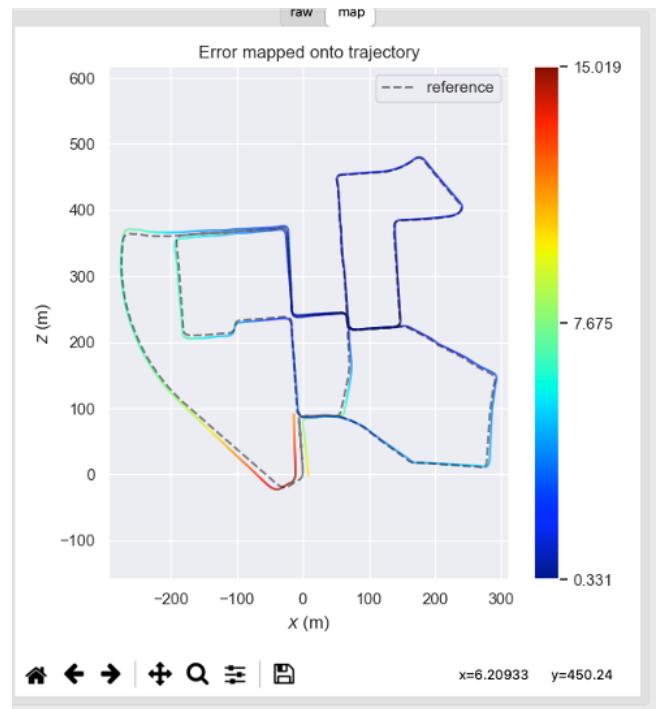
### 4.1 The Open Dataset

For the odometry part, we evaluate the algorithm on the kitti dataset, which is one of the most famous auto driving dataset in the world. We use the evo tools to analysis the trajectory

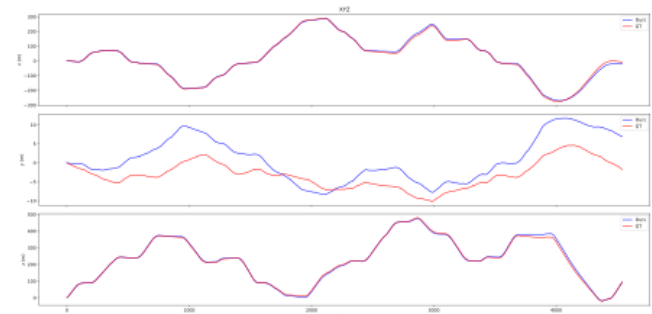
The Figure 6 and Figure 7 shows the whole trajectory performance and the drift of three different axis. From the results, we can see that the estimated odometry is close to the ground truth. Furthermore, to analysis the influence of different feature types, we do the ablation study of them. We separately use the point or surf features to estimate the drift of odometry and compare it to the ground truth. The result is shown in Figure 6:

Table 1 shows that the point features are better than the surf features. From deeply study, the poor surf feature results is mainly suffered from the mismatch correspondences, but the ground plane is an important factor to estimate the sensor’s height. With the deep study, we could use different weights to get better results. From the test, we could see that when the environment covered with more trees, bushes, the point feature factors should be increased and vice versa. In this test, we should change point factor as 0.6317 and the surf factor as 0.3683. After that, the better result is 1.2445% drift.

As mentioned above, in terms of the reconstruction quality, we evaluate the thickness of the reconstruction results. The whole result is shown below Figure 8:



**Figure 6.** The whole trajectory evaluation



**Figure 7.** The drift on the different axis

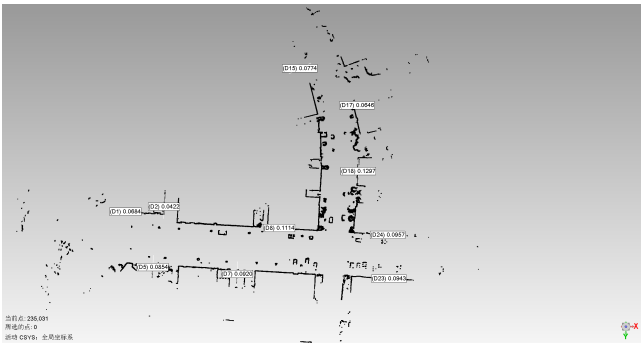


**Figure 8.** The reconstruction result of kitti dataset. From the thickness perceptive, the reconstruction of kitti environment has a better result.

From the industry experience, the thickness less than 10 cm represents that the reconstruction results has a better result. So we can see that the algorithm can have a great reconstruction result on the open dataset.

#### 4.2 Experiment on the Power Transmission Site

To evaluate our algorithm on the real power site environment, we use the equipment(Fig.9) to collect data in the real power transmission site. The reconstruction result is shown in the fig.10.

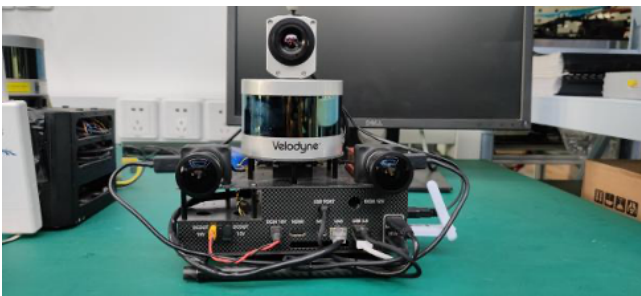


**Figure 9.** The data collecting equipment

The reconstruction result is shown in Figure 11:

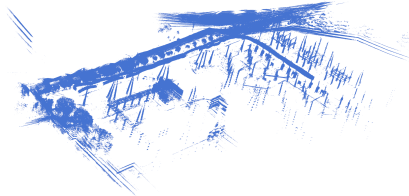


**Figure 10.** The reconstruction result of the power site without ground plane information.

Because of the lack of GNSS devices in our equipment, so we only use the thickness of the point cloud reconstruction to show the reconstruction quality.

Like Fig. 13. shows, the reconstruction result has a better reconstruction quality. We use the reconstruction result to split out the training data used for the tree's height detection. The detection algorithm we used is PointNet. The Splitting data is shown below:

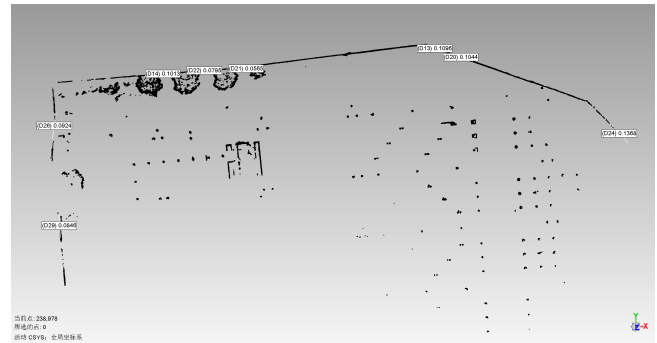


**Figure 11.** The analysis of power site reconstruction from the thickness perceptive. The reconstruct result is suitable for vegetation management.

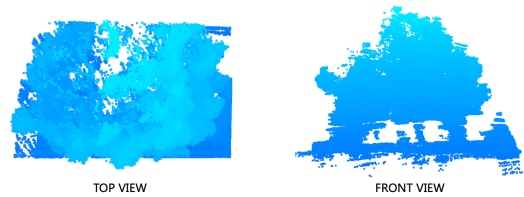


**Figure 12.** Wrong Split Results. The Segmented tree has the messy ground plane.

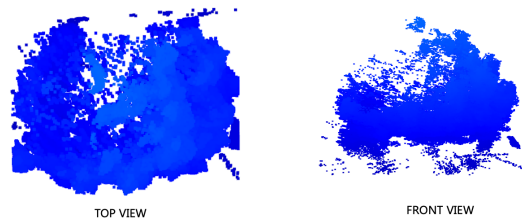


**Figure 13.** Correct Split Results. The Segmented tree without messy ground plane is more clean

In order to show the messy ground plane influence. We use the split data from two reconstruction result and train it to detect the tree's height separately. We label the tree name as Figure 14 to make a clear comparison. The detection results with messy ground plane training data would mis-detect some points on the ground plane as the tree, while the correct split training data has a better detection results. The comparison results are shown in Figure 12 and Figure 13.

With two different reconstruction result as training data, the whole detection result is shown like the table 2. We use the detected bounding box to calculate the tree's height and the ground truth of the tree's height is measured by the electronic total station. The tree 1 to tree 4 are the general formed trees and the tree 5 to tree 10 are the trees with messy trunks. We split out the tree 8, which is the tree with messy trunks, to make the comparison. The height detection from without ground plane reconstruction is 5.127m and the detection with ground plane reconstruction is 5.163m. The table 2 shows that the height detection of two reconstructions result is close to each other, it mainly caused by the different training size and the different training steps. However, from the result, tree 5 tree 10, our reconstruction result has a better accuracy which proves that our system is more robustness and accurate.

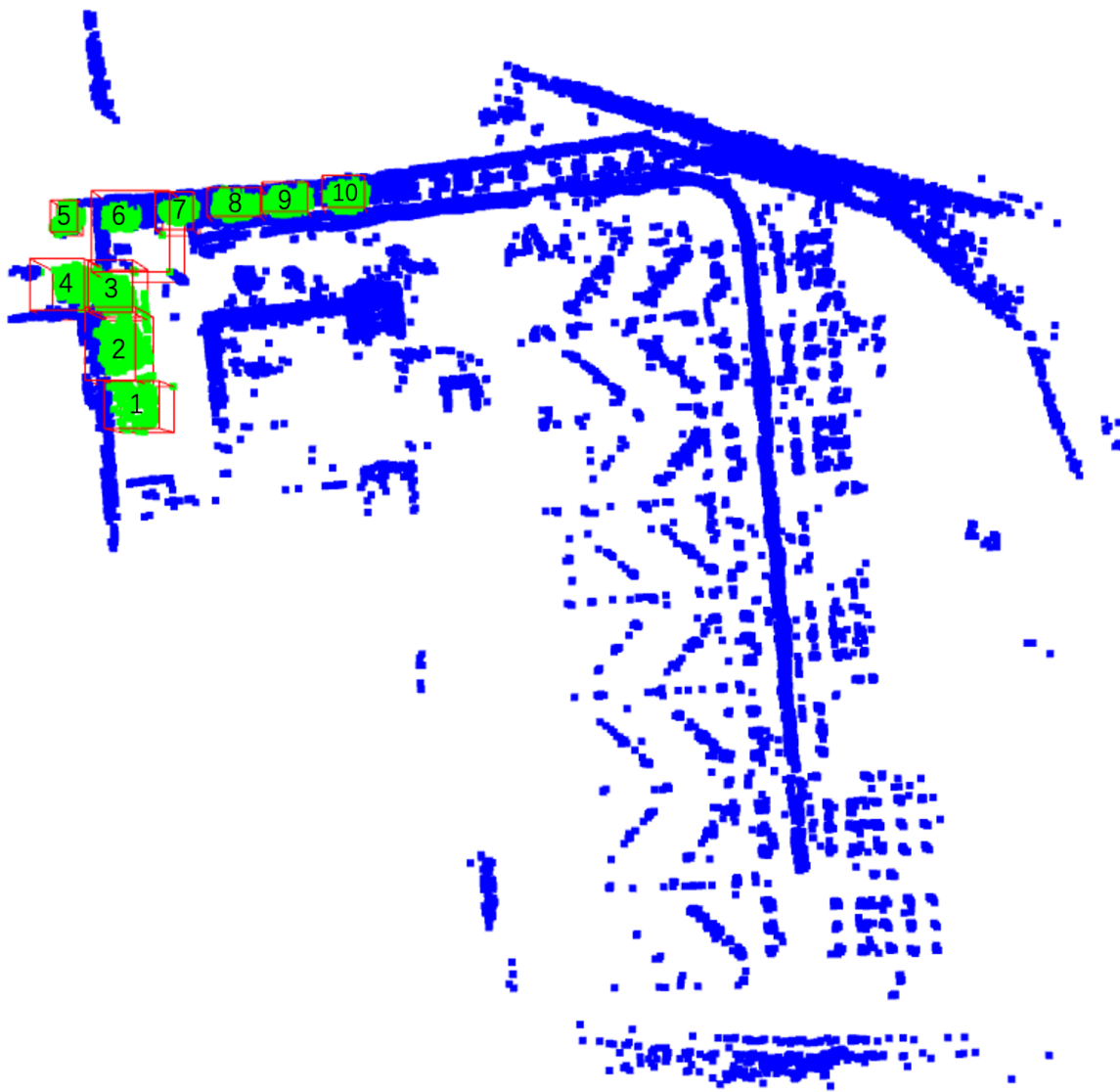


**Figure 14.** The label of each tree. There are about ten tree in the power site, the detection of different reconstruction results are shown in the table 2 and the figure 16 and 17

**Table 2.** The Detection Of Tree Height

The Reconstruction Result	Tree 1	Tree 2	Tree 3	Tree 4	Tree 5	Tree 6	Tree 7	Tree 8	Tree 9	Tree 10
The Tree Height With Ground Plane	7.506	12.295	<b>7.1785</b>	<b>8.355</b>	7.766	<b>7.907</b>	4.167	5.163	4.724	5.808
The Tree Height Without Ground Plane	<b>7.713</b>	<b>9.035</b>	7.431	8.973	<b>2.437</b>	8.044	<b>4.141</b>	<b>5.127</b>	<b>4.843</b>	<b>5.505</b>
The Ground Truth Of Tree Height	7.693	10.123	7.144	8.652	2.535	7.524	7.853	4.535	4.824	5.437

## 5. CONCLUSIONS

In this paper, we propose a reconstruction system used for tree's height detection in power site environment. We use the concentric-zone model to effectively remove the ground plane noise and the reconstruction results show that deep-learning methods used our reconstruction result is more accurate and effective. Experiment results proved that our reconstruct system is more suitable for the tree's height detection task, which is useful in the electric industry. In future, we would improve the reconstruction system to more semantic tasks for the vegetation management.

## ACKNOWLEDGEMENTS

The author's work are supported by the project (No.YNKJXM20191246) on the research and application of constructing satellite remote sensing technology power application comprehensive test site and environment wide area intelligent monitoring.

## REFERENCES

Ali, W., Abdelkarim, S., Zidan, M., Zahran, M., El Sallab, A., 2018. Yolo3d: End-to-end real-time 3d oriented object bounding box detection from lidar point cloud. *Proceedings of the*

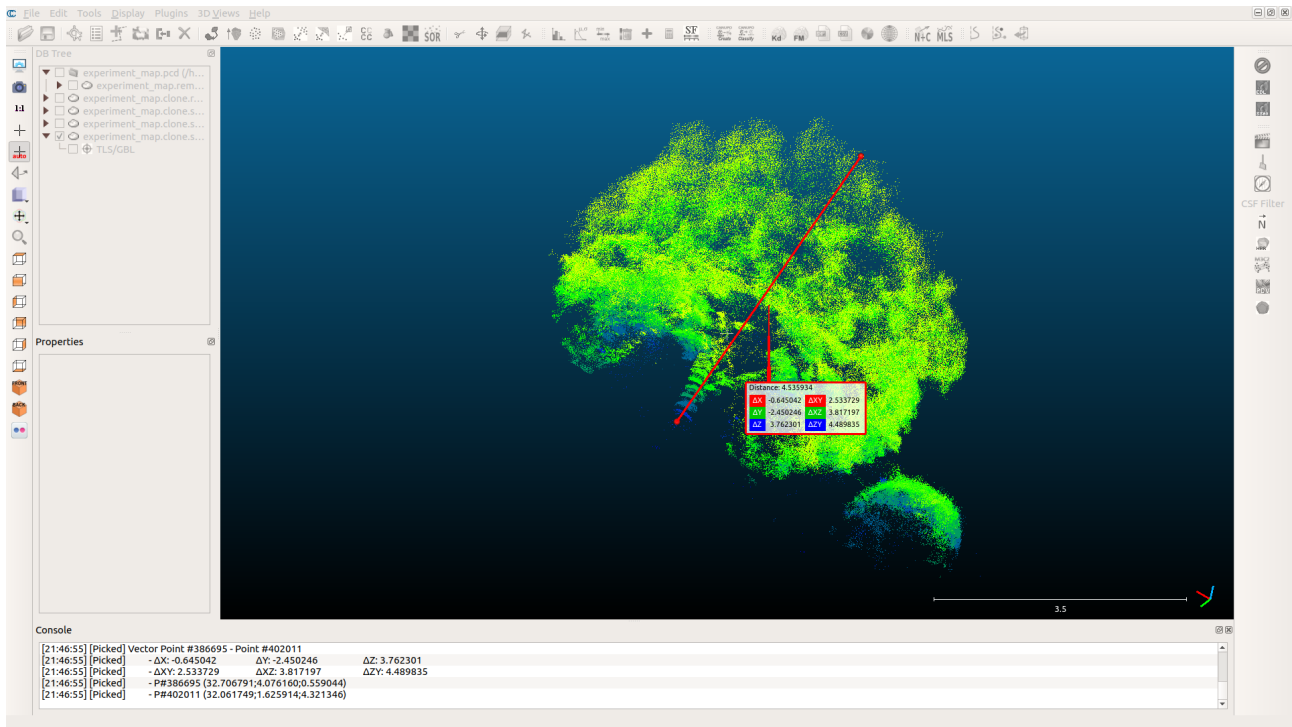


**Figure 15.** The example detection height of tree 8 height is 4.535m

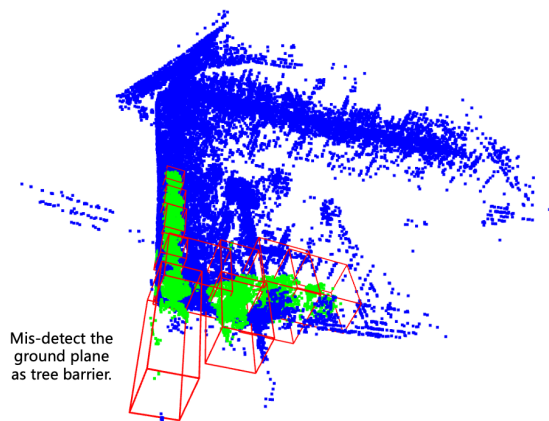


**Figure 16.** The detection results with ground plane reconstruction. The detection result of tree5 has messy ground plane noise.

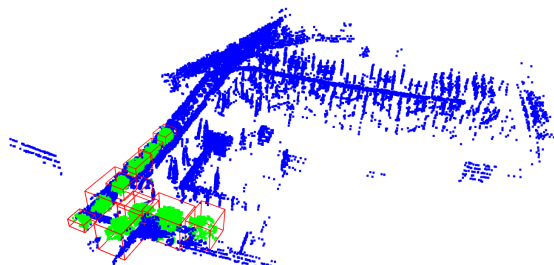


**Figure 17.** The detection results with training data without ground plane. The detection results of tree5 is more clean.

*European Conference on Computer Vision (ECCV) Workshops*, 0–0.

Bogoslavskyi, I., Stachniss, C., 2016. Fast range image-based

segmentation of sparse 3d laser scans for online operation. *2016 IEEE/RSJ International Conference on Intelligent Robots and Systems (IROS)*, IEEE, 163–169.

Chen, T., Dai, B., Wang, R., Liu, D., 2014. Gaussian-process-based real-time ground segmentation for autonomous land vehicles. *Journal of Intelligent & Robotic Systems*, 76(3), 563–582.

Cheng, J., He, D., Lee, C., 2020. A simple ground segmentation method for lidar 3d point clouds. *2020 2nd International Conference on Advances in Computer Technology, Information Science and Communications (CTISC)*, IEEE, 171–175.

Deschaud, J.-E., 2018. Imls-slam: scan-to-model matching based on 3d data. *2018 IEEE International Conference on Robotics and Automation (ICRA)*, IEEE, 2480–2485.

Himmelsbach, M., Hundelshausen, F. V., Wuensche, H.-J., 2010. Fast segmentation of 3d point clouds for ground vehicles. *2010 IEEE Intelligent Vehicles Symposium*, IEEE, 560–565.

Jelavic, E., Jud, D., Egli, P., Hutter, M., 2021. Towards Autonomous Robotic Precision Harvesting: Mapping, Localization, Planning and Control for a Legged Tree Harvester. *Field Robotics*.

Lim, H., Oh, M., Myung, H., 2021. Patchwork: concentric zone-based region-wise ground segmentation with ground likelihood estimation using a 3D LiDAR sensor. *IEEE Robotics and Automation Letters*, 6(4), 6458–6465.

Milioto, A., Vizzo, I., Behley, J., Stachniss, C., 2019. Rangenet++: Fast and accurate lidar semantic segmentation. *2019 IEEE/RSJ International Conference on Intelligent Robots and Systems (IROS)*, IEEE, 4213–4220.

Qi, C. R., Su, H., Mo, K., Guibas, L. J., 2017. Pointnet: Deep learning on point sets for 3d classification and segmentation.

*Proceedings of the IEEE conference on computer vision and pattern recognition*, 652–660.

Shan, T., Englot, B., 2018. Lego-loam: Lightweight and ground-optimized lidar odometry and mapping on variable terrain. *2018 IEEE/RSJ International Conference on Intelligent Robots and Systems (IROS)*, IEEE, 4758–4765.

Zhang, J., Singh, S., 2014. Loam: Lidar odometry and mapping in real-time. *Robotics: Science and Systems*, 2number 9.

Zhang, J., Singh, S., 2017. Low-drift and real-time lidar odometry and mapping. *Autonomous Robots*, 41(2), 401–416.

Zhou, P., Guo, X., Pei, X., Chen, C., 2021. T-LOAM: Truncated Least Squares LiDAR-Only Odometry and Mapping in Real Time. *IEEE Transactions on Geoscience and Remote Sensing*.